Crystallization and structural properties of a family of isotopological 3D-networks: the case of 4,4'-bipy ligand – M^{2+} triflate system.

Silvia Rizzato,[*a] Massimo Moret,[*b] Fabio Beghi[a] and Leonardo Lo Presti[a,c,d]

[a] *Università degli Studi di Milano, Dipartimento di Chimica, via Golgi 19, I-20133 Milano, Italy*

[b] *Università degli Studi di Milano Bicocca, Dipartimento di Scienza dei Materiali, via Cozzi 55, I-20125 Milano, Italy*

[c] *Centre for Materials Crystallography, Århus University, Langelandsgade 140, 8000 Århus, Denmark*

[d] *CNR-ISTM, via Golgi 19, I-20133 Milano, Italy*

AUTHOR EMAIL ADDRESS silvia.rizzato@unimi.it

ELECTRONIC SUPPLEMENTARY INFORMATION

(ESI)

S1. X-ray Single-Crystal Structural Determination.

The crystal data for all the compounds are listed in Table 1. The data collections were performed at 293 K (CUT-**1b**, CUT-**1c**, FET-**4**), 120 K (CUT-**1a**, FET-**2**), 150 K (CDT-**3**) using graphite-monochromated Mo Kα radiation (λ = 0.71073 Å) on a Bruker SMART Apex diffractometer equipped with a CCD detector and an Oxford Cryosystems N_2 gas blower. ω-scans were performed throughout at a nominal X-ray power of 50 kV x 30 mA, within Bragg limits of 1.95° < θ < 24.83° (CUT-**1a**), 1.43° < θ < 26.62° (CUT-**1b**), 1.93° < θ < 19.99° (CUT-**1c**), 1.92° < θ < 23.97° (FET-**2**), 1.88° < θ < 29.63° (CDT-**3**), 2.22° < θ < 23.26° (FET-**4**). Determination of the integrated intensities and unit cell refinements were performed using SAINT[1] and all absorption corrections were applied by using SADABS.[2] The structures were solved by direct methods (SIR2004)[3] and refined by full-matrix least squares on F^2 (SHELX 2014)[4] with the WINGX interface.[5]

In all structures, except FET-**4**, hydrogen atoms were placed in geometrically calculated positions and included in the refinement using a riding model in conjunction with a $U_{iso}(H) = 1.2\ U_{eq}(-CH_2, -CH)$ constraint. No hydrogen atoms were assigned to guest molecules in CUT-**1a**. In FET-**4** all hydrogen atoms were located from the difference Fourier map and their geometric parameters were refined applying SADI restraints[4] for water molecules on O-H distances, with $U_{iso}(H) = 1.5\ U_{eq}$ (O) for water. A $U_{iso}(H) = 1.2\ U_{eq}$ (C) constraint was instead used for H-bipy.

In CUT-**1b**, CUT-**1c** and FET-**2** the data were corrected for disordered residual electron density, probably due to the contributions of disordered solvent, by using the SQUEEZE procedure as implemented in PLATON program.[6]

Bipy ligands and Cu atoms were refined in all structures with full occupancy and anisotropic displacement parameters. The only exception is CUT-**1c**, where the ligand is positionally disordered over two chemically equivalent sites. The two possible arrangements were explicitly accounted for in the least-squares model, assigning to each atom a halved site-occupancy factor. Due to the poor intensity statistics of high-angle data (Table 1), isotropic displacement parameters were used for all non-H atoms in this structure to cope with the unfavourable data-to-parameter ratio.

Coordinated trifluoromethanesulfonate anions were found to be disordered in compounds CUT-**1a**, CUT-**1b**, FET-**2**, CDT-**3** and FET-**4** and were refined over two positions using suitable models (1a: 79 %; 1b: 62%; 2: 53%; 3: 54%-61%; 4: 56%). Hereinafter, we will refer as "model A" to the structure bearing disordered moieties with the highest occupancy, and as "model B" to that corresponding to the lowest one. Several soft constraints and restraints were applied in the refinements to get reasonable geometrical and thermal parameters. In CDT-**3**, one of the two symmetry-independent SO_3CF_3 anions was found to be disordered over a metal-coordinated and uncoordinated state. A static positional disorder model was thus considered; a water molecule was assumed as an alternative ligand for the free coordination site. Complementary occupancy factors refined to 62 % (coordinated triflate) and 38 % (coordinated water). Anisotropic displacement parameters were explicitly considered just for the major component.

Several weakly observed guest molecules were found in the structures CUT-**1a** (water and THF) and CDT-**3** (CH_2Cl_2, THF), showing either positional (water, CH_2Cl_2) or rotational (THF) disorder, typically over two different crystallographic sites. The guest species were refined isotropically with suitable partial site-occupancy factors, taking into account the multiplicity of special positions when needed. Geometry constraints (SADI) were used to maintain reasonable molecular geometries of THF (in CUT-**1a**) and dichloromethane (in CDT-**3**). Solvent H atoms were added in calculated positions and refined only in CDT-**3**. The final least-squares models had reasonable thermal parameters and acceptable agreement statistics (Table 1).

Figure 1S. Rotation of the triflate groups about the bond between the sulfur and the coordinated oxygen that is pointed out by the increase of about 20° of the Cu-O-S-C torsion angle. a) CUT1a, b) CUT1b, c) CUT1c.

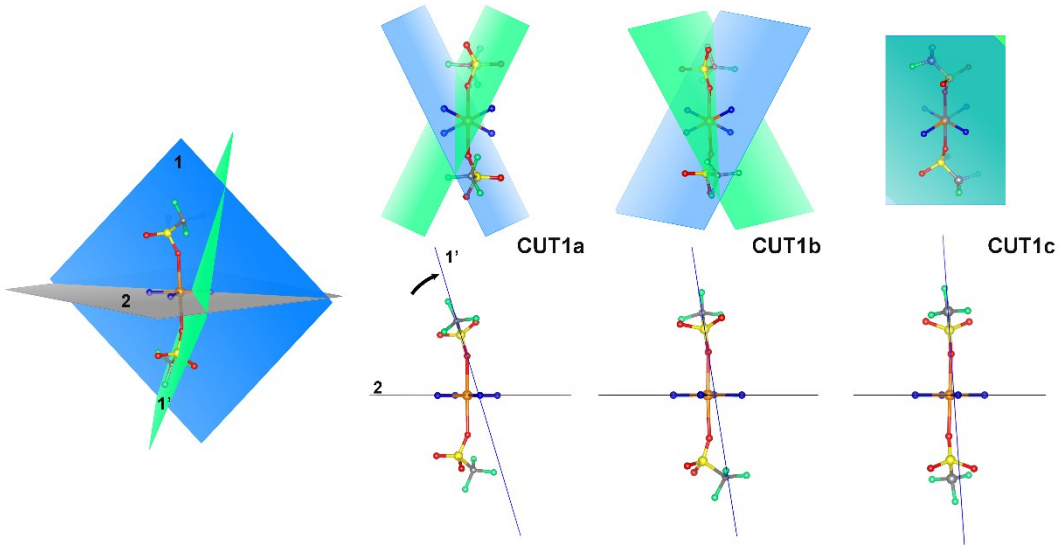

Figure 2S. Reorientation of the triflate anions in the copper coordination sphere described by the variation of the dihedral angles between the planes defined by the two O-S-C groups, that is plane 1 (blue) and plane 1' (green), and the CuN_4 plane, labelled plane 2 (grey). Top: variation of the 1 ^ 1' angle, whose final value confirm the final parallel arrangement of the two triflates (1 ^ 1' = 0). Bottom: variation of the 1 ^ 2 angle.

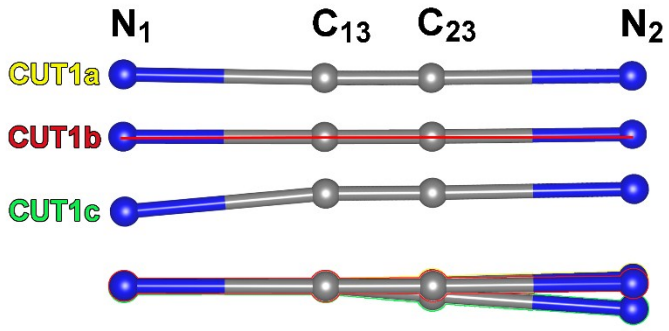

Figure 3S. Slight bending of the molecule during the empting process described by the changes of the angles involving the nitrogen atoms and the opposite carbon atoms of the rings (Table 3: angle N_1-C_{13}-N_2; angle N_2-C_{23}-N_1).

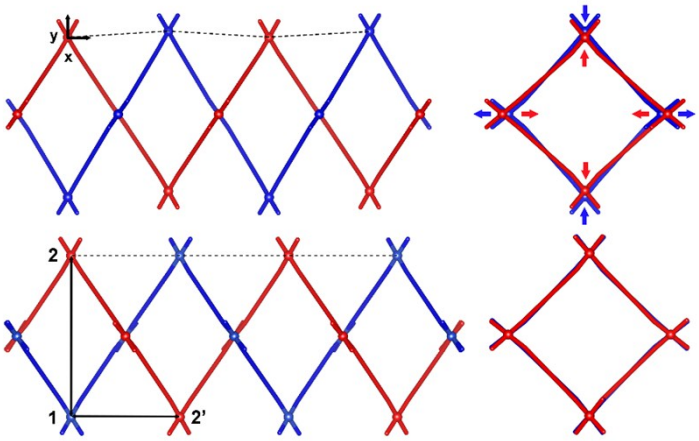

Figure 4S. Changes in the double helices as result of the dehydration process. Top: at first, the two intertwined helices (in blue and red) show a later shift of the nodes described by the value of x and y parameter. Moreover, the rhombic mouths of the channels appear rotated by 90°. During the emptying process of the network, the pitches of the helices lengthen while their diameters narrow down to the same degree but in opposite direction. The changes of some geometrical parameters, like the 1-2 and 1-2' distances, that shorten and lengthen respectively, allow to schematically describe the modification involving the double helices. At the end (bottom), the channel openings became square and perfectly overlapped.

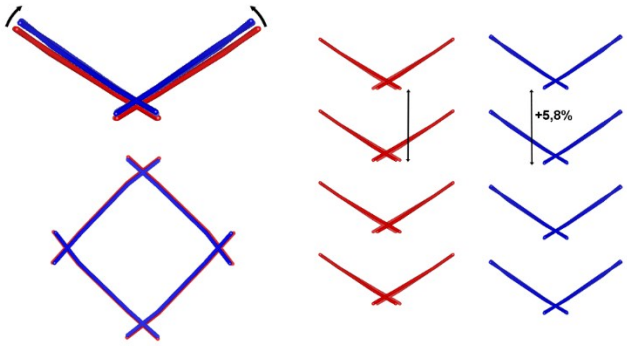

Figure 5S. Increase of the bending angle of the rhombic meshes resulting in a very small constriction of the square openings of the channels and a moving away of the elements along the stacking direction.

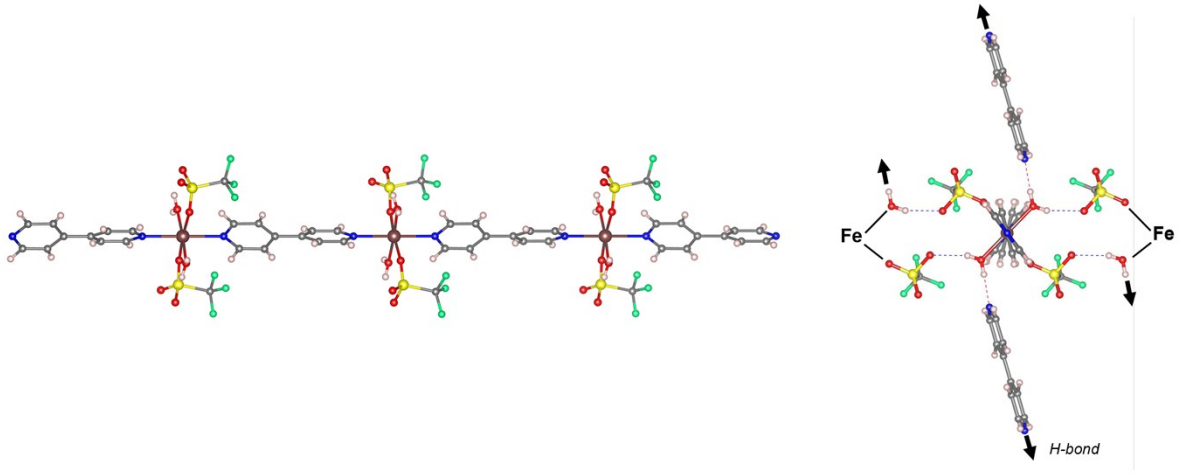

Figure 6S. Compound $[Fe(bipy)(H_2O)_2\ (SO_3CF_3)_2]\cdot(bipy)$ (FET-**4)** consists of 1D metal chains running along the **c** axis, with the uncoordinated bipy molecules involved in hydrogen bonds with the coordinated water molecules. Compounds FET-**4** is isostructural and isomorphous to CDT-**5** polymer (reported elsewhere).[7] Left: a side view of a one-dimensional polymer chain. Right: a schematic view of the coordination environment around the iron cation showing all the hydrogen bonds involving the coordinated water molecules and triflate anions and the uncoordinated bipy ligands (D···A distances: O1w-H1w···O3A: 2.852(12) Å; O1w-H2w···N3: 2.737(8) Å). The H-bonds connect the chains to form a three-dimensional supramolecular network.

Table 1S. Selected bond distances (Å) and angles (°) in compounds CUT-**1a**, CUT-**1b**, CUT-**1c**, FET-**2** and CDT-**3**.

CUT-**1a**		CUT-**1b**		CUT-**1c**		FET-**2**		CDT-**3**	
Cu-N1	2.010 (3)	Cu-N1	2.033 (4)	Cu-N1	2.052 (7)	Fe-N1	2.173 (4)	Cd-N1	2.299 (4)
Cu-N2	2.027 (3)	Cu-N2	2.040 (4)	Cu-N2	2.013 (7)	Fe-N3	2.174 (4)	Cd-N2	2.325 (4)
Cu-O1	2.452 (3)	Cu-O1	2.506 (9)	Cu-O1	2.386 (9)	Fe-N4	2.190 (4)	Cd-N3	2.312 (4)
						Fe-N2	2.198 (5)	Cd-N4	2.310 (4)
						Fe-O11a	2.078 (14)	Cd-O11	2.340 (5)
						Fe-O21	2.098 (4)	Cd-O21	2.331 (5)
CUT-**1a**		CUT-**1b**		CUT-**1c**		FET-**2**		CDT-**3**	
N1-Cu-N2	178.97 (14)	N1-Cu-N2	178.30 (17)	N1-Cu-N2^{ii}	88.6 (4)	N1-Fe-N4	92.56 (16)	N1-Cd-N2''	178.02 (17)
N1-Cu-N1^{i}	91.7 (2)	N1^{i}-Cu-N1	93.1 (2)	N1-Cu-N2	91.4 (4)	N1-Fe-N2	178.31 (16)	N1-Cd-N3	92.16 (16)
N1-Cu-N2^{i}	89.29 (14)	N1^{i}-Cu-N2	88.62 (17)	N1-Cu-N1^{ii}	180.0 (4)	N1-Fe-N3	91.81 (15)	N1-Cd-N4'	91.81 (17)
N2^{i}-Cu-N2	89.7 (2)	N1-Cu-N2^{i}	88.62 (17)	N2-Cu1-N1^{ii}	91.4 (4)	N3-Fe-N2	86.51 (16)	N3-Cd-N2''	85.96 (16)
N1^{i}-Cu-N2	89.29 (14)	N2-Cu-N2^{i}	89.7 (2)	N2-Cu1-N1^{ii}	88.6 (4)	N3-Fe-N4	175.56 (15)	N4'-Cd-N2''	90.06 (17)
N1-Cu1-O1	90.7 (1)	N1-Cu1-O1	89.8(4)	N1-Cu1-O1	87.9 (3)	N4-Fe-N2	89.12 (16)	N4'-Cd-N3	175.87 (16)
N2-Cu1-O1	88.98 (13)	N2-Cu1-O1	90.6(4)	N2-Cu1-O1	87.7 (3)	O11A-Fe-O21	177.1 (5)	O21-Cd-O11	175.17 (18)
						O11A-Fe-N1	90.5 (5)	N1-Cd-O11	89.42 (19)
						O11A-Fe-N2	89.4 (5)	N2''-Cd-O11	89.90 (19)
						O11A-Fe-N3	91.5 (5)	N3-Cd-O11	88.60 (19)
						O11A-Fe-N4	87.7 (4)	N4'-Cd-O11	90.31 (19)
						O21-Fe-N1	89.32 (17)	N1-Cd-O21	91.20 (18)
						O21-Fe-N2	90.88 (16)	N2''-Cd-O21	89.63 (19)
						O21-Fe-N3	91.41 (17)	N3-Cd-O21	96.16 (18)
						O21-Fe-N4	89.45 (16)	N4'-Cd-O21	84.88 (18)

Symmetry codes: (i) -*x*+3/2, *y*, -*z*; (ii) -*x*+3/2, -*y*+1/2, -*z*+3/2; (') *x*+1/4, *y*+1/4, -*z*; ('') *x*-1/4, -*y*, *z*-1/4

Table 2S. Relevant torsion angles (degrees), bond angles (°) and bond lengths (Å) describing the orientation of the coordinated triflate anions in FET-**2** and CDT-**3**. Labels t_1 and t_2 concern the orientation of triflate groups (see Figure 3) and are related to 1 ^ 1' and 1 ^ 2, which quantify the dihedral angles shown in Figure 2S. Estimated standard deviations are given in parentheses only for bond angles and lengths.

TRIFLATE	torsion/dihedral angle (°)							bond angle (°)		bond length
	N-Cu-O-S		**Cu-O--S-C**	**C-S… …S-C**	**S-O… …O-S**	**Angle 1 ^ 1'**	**angle 1 ^ 2**	**Cu-O-S**	**O-S-C**	**S-C**
	t_1	**t_2**								
FET-**2**	79.8	-18.1	-132.3	172.4	-64.0	45.3	73.6	154.9(11)	109.0(8)	1.67(2)
			-134.3				72.2	154.9(3)	104.0(4)	1.768(9)
CDT-**3**	-147.8	-15.8	-131.4	-147.6	-166.8	29.0	80.9	163.5(4)	107.1(7)	1.84(2)
			144.7				66.9	143.3(3)	97.5(5)	1.88(2)

Table 3S. Relevant geometrical angles (°), geometrical lengths and bond lengths (Å) involving the bipy ligand linkers in FET-**2** and CDT-**3** (see Figure 3S for). β represents dihedral angles between the pyridyl planes within the same bipy moiety. Estimated standard deviations are given in parentheses for bond lengths.

LIGAND		**d (M-N)**	**d (N-N)**	**d (M-M)**	**β**	**Cu-N_X-C_{X3}**	**N_X-C_{X3}-N_Y**	**M-N-N**
FET-**2**	L1	2.173(4); 2.198(5)	7.059	11.426	34.0	177.0; 177.9	178.9; 178.7	177.6; 177.6
	L2	2.174(4); 2.190(4)	7.073	11.389	37.7	168.4; 179.2	177.4; 178.2	177.4; 178.2
CDT-**3**	L1	2.299(4); 2.325(4)	7.064	11.688	33.8	179.6; 179.0	179.5; 179.3	179.5; 179.0
	L2	2.310(4); 2.312(4)	7.050	11.603	38.4	166.3; 176.8	177.3; 177.5	164.7; 176.9

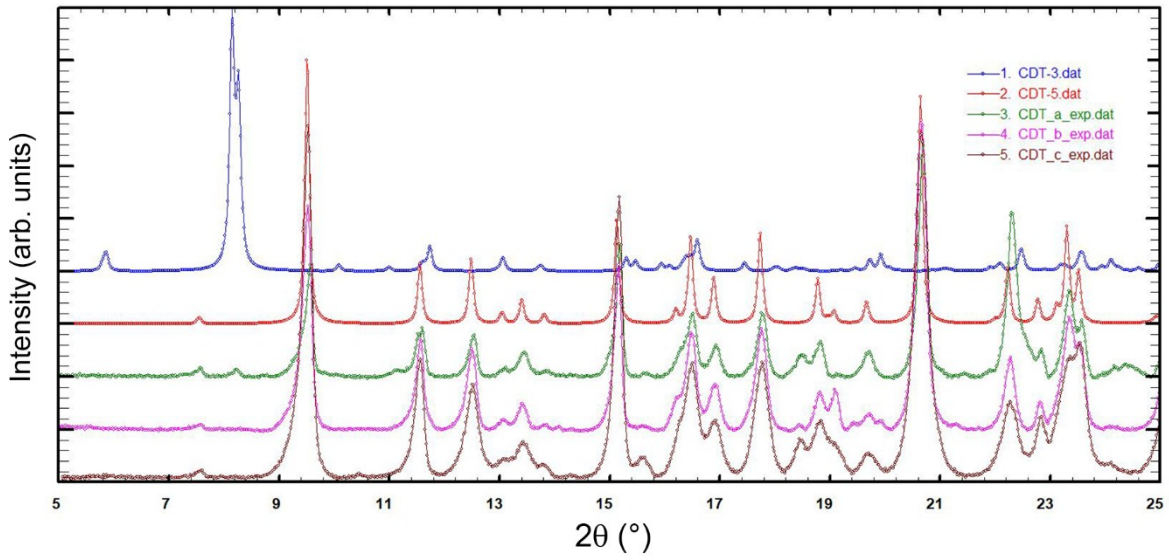

FIGURE 7S.
Comparison between experimental *and* simulated powder X-ray diffraction *(*XRD*)* patterns for the Cd-bipy system. CDT-3 (blue line) and CDT-5 (red line) are the spectra simulated from the single-crystal structure data of the two Cadmium 3D (CDT-3) and 1D (CDT-5) networks.
The patterns CDT_a_exp, CDT_b_exp, CDT_c_exp refer to experimental data collected on powder samples prepared as follow:
a) Large part of the crystalline material precipitated in the crystallization batch containing the single crystals of CDT-3 and CDT-5 species (see experimental section) was recovered by filtration, dried in air and gently *grounded* in an agate *mortar.*
b) 15 mL of a 80 mM solution of bipy (186.7 mg; 1.195 mmol) in CH_2Cl_2 were added to 15 mL of a 41 mM solution of $Cd(SO_3CF_3)_2{\cdot}6H_2O$ (318.7 mg; 0.614 mmol) in THF (M:L ratio 1:2). The mixture was stirred for 3 hours and then left to stand overnight at room temperature. The resulting white precipitate was recovered by suction filtration and dried in air at room temperature. The sample was hand-grounded using an agate mortar before performing XRD data analysis.
c) 3 mL of a 80 mM solution of bipy (37.6 mg; 0.241 mmol) in THF were added to 15 mL of a 40 mM solution of $Cd(SO_3CF_3)_2{\cdot}6H_2O$ (62.5 mg; 0.120 mmol) in THF (M:L ratio 1:2). The mixture was stirred for 5 hours and then left to stand overnight at room temperature. The resulting white precipitate was recovered by suction filtration and dried in air at room temperature. The sample was hand-grounded using an agate mortar before performing XRD data analysis.

The same results have been also obtained by using different reactants concentrations and/or metal-ligand molar ratio. The comparison shows clearly that all the experimental spectra are in close agreement with the simulated pattern of the pure CDT-5 compound. These results confirm the structural instability of the porous CTD-3 network that transforms into the CDT-5 phase when removed from the mother liquor and consequently the infeasibility to obtain the CDT-3 specie in pure bulk form.

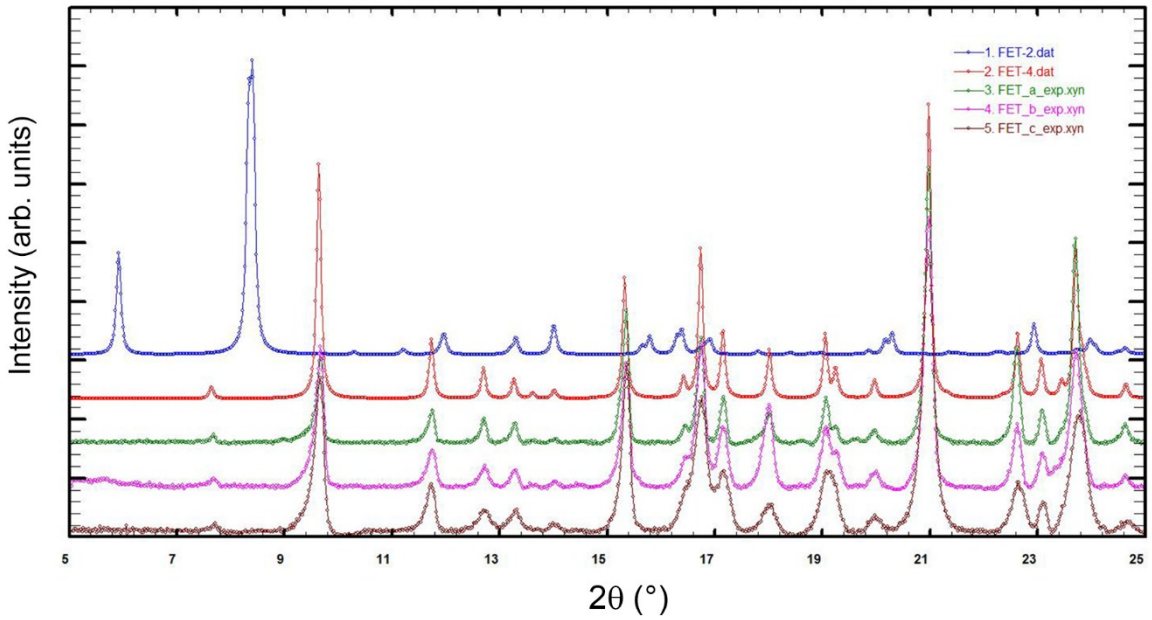

FIGURE 8S.
Comparison between experimental and simulated powder X-ray diffraction *(*XRD*)* patterns for the Fe-bipy system. FET-2 (blue line) and FET-4 (red line) are the spectra simulated from the single-crystal structure data of the two iron 3D (FET-2) and 1D (FET-4) networks.
The patterns FET_a_exp, FET_b_exp, FET_c_exp refer to experimental data collected on powder samples prepared as follow:
a) Some large crystals of FET-2 specie, readily recognizable from their morphology, were carefully selected under an optical microscope and placed on a paper filter disk to remove the excess of solvent. The sample was gently grounded in an agate mortar before performing XRD data analysis.
b) 50 mL of a 61 mM solution of bipy (476.7 mg; 3.052 mmol) in CH_2Cl_2 were added to 50 mL of a 30 mM solution of $Fe(SO_3CF_3)_2{\cdot}6H_2O$ (695.43 mg; 1.505 mmol) in THF (resulting M:L ratio 1:2). The mixture was stirred for about 30 minutes and then left to stand overnight at room temperature. The resulting yellow precipitate was recovered by gravity filtration and dried in air at room temperature. The sample was hand-grounded using an agate mortar before performing XRD data analysis.
c) 4 mL of a 15 mM solution of $Fe(SO_3CF_3)_2{\cdot}6H_2O$ (27.3 mg; 0.059 mmol) in THF was layered onto 4 mL of a 30 mM solution of bipy (28.0 mg; 0.116 mmol) in THF (M:L ratio 1:2). The mixture was left to stand for some hours at room temperature and then filtered under vacuum. The resulting yellow precipitate was dried in air at room temperature and hand-grounded using an agate mortar before performing XRD data analysis.

The comparison shows clearly that all the experimental spectra are in close agreement with the simulated pattern of the pure FET-5 compound. Similarly to what observed for the Cd-system, the results confirm the structural instability of the porous FET-2 network.

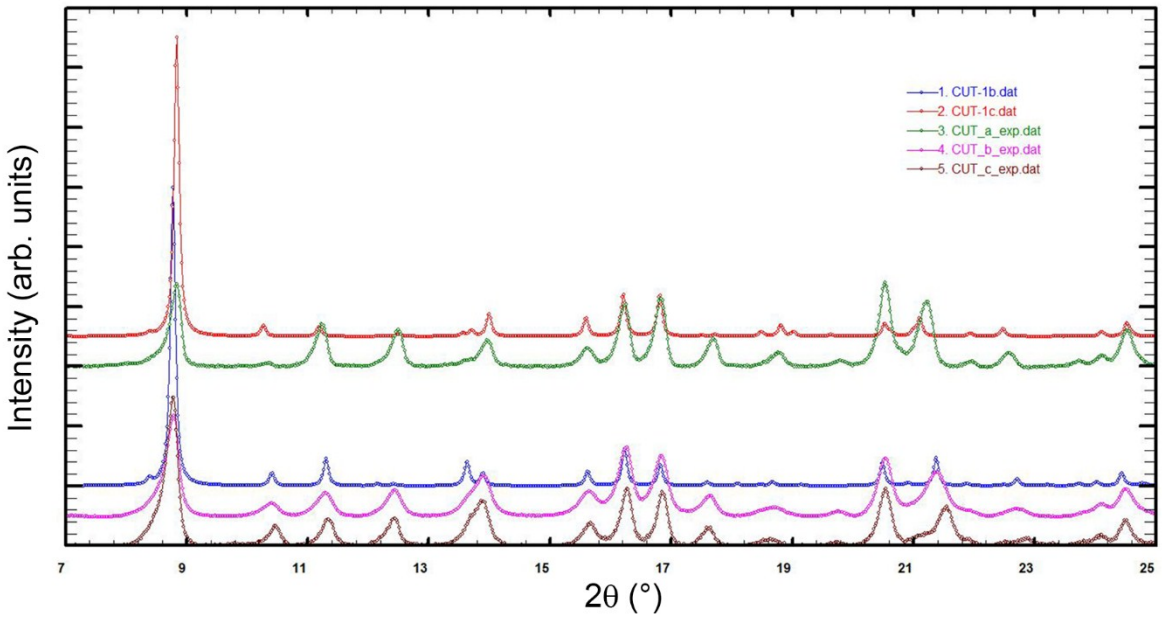

FIGURE 9S.
Comparison between experimental and simulated powder X-ray diffraction *(*XRD*)* patterns for the Cu-bipy system. CUT-**1b** (blue line) and CUT-**1c** (red line) are the spectra simulated from the single-crystal structure data of the partially (**1b**) and almost full dehydrated (**1c**) 3D network respectively.
The patterns CUT_a_exp, CUT_b_exp, CUT_c_exp refer to experimental data collected on powder samples prepared as follow:
a) 100 mL of a 59.6 mM solution of bipy (931.4 mg; 59.6 mmol) in CH_2Cl_2 were added to 100 mL of a 30 mM solution of $Cu(SO_3CF_3)_2$ (1086.1 mg; 3.0 mmol) in THF (resulting M:L ratio 1:2). The mixture was stirred for about 2 hours and then left to stand overnight at room temperature. The resulting pale blue precipitate was recovered by gravity filtration and dried in air at room temperature. The sample was hand-grounded using an agate mortar before performing XRD data analysis.
b) Powder of *b* sample was prepared with same procedure as described above for *a* sample by using the following solutions: 3 mL of a 100.0 mM solution of bipy (46.8 mg; 0.30 mmol) in THF and 3 mL of a 50.1 mM solution of $Cu(SO_3CF_3)_2$ (1086.1 mg; 3.0 mmol) in THF (resulting M:L ratio 1:2).
c) 3 mL of a 31.8 mM solution of bipy (14.9 mg; 0.095 mmol) in THF was layered onto 3 mL of a 15.8 mM solution of $Cu(SO_3CF_3)_2$ (17.1 mg; 0.150 mmol) in THF (M:L ratio 1:2). The mixture was left to stand for some days at room temperature and then filtered under vacuum. The resulting pale blue precipitate was dried in air at room temperature and hand-grounded using an agate mortar before performing XRD data analysis.

The comparison shows clearly that all the experimental spectra are in close agreement with the simulated patterns of the pure CUT-**1** compound partially (for sample *a*) or almost fully (for samples *b* and *c*) dehydrated.

A lot of crystallization trials have been performed employing THF or THF/CH_2Cl_2 as solvent system by changing systematically the concentrations of the reactants and/or the metal-to-ligand molar ratio. The nature of all powder samples has been checked by XRPD methods. In all cases the experimental data are in good agreement with calculated ones from the single-crystal structure of CUT-**1** compound.

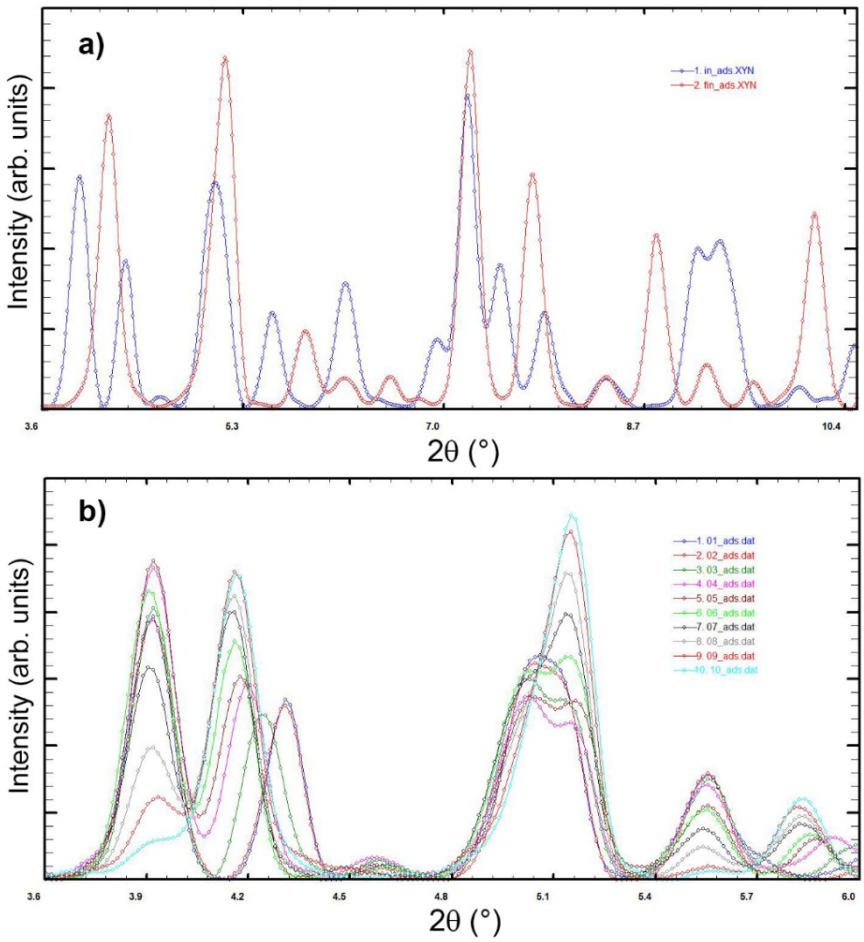

FIGURE 10S.

In-situ time-resolved X-ray powder diffraction patterns on the compound CUT-**1** were collected by using synchrotron radiation at the GILDA-BM08 beamline of ESRF (Grenoble, France) has allowed to study the structural modifications taking place in the CUT-**1** porous coordination polymer during the uptake process of vapours of volatile organic compounds. The full analysis of the data will be published elsewhere but it is possible to anticipate some meaningful insights provided by this study about the inclusion process of the guest molecules and clarifying some details of previously unexplained findings, that is:[8]

- the dynamic behaviour of the network during the solvation/desolvation process is strongly dependent from the size, geometry and chemical nature of the guest molecules as revealed by the non-identical trend in the variation of the unit cell volume and lattice parameters accompanying the guest inclusion/release (a marked lengthening of the c axis accomplished by a small shortening of a/b axes or a decrease of c accomplished by a modest increase of a/b) probably due to a different distribution of the guest molecules in the helical channels or in the interchannel regions.
- the unexpected distortion behaviour occurring upon adsorption of nitromethane observed by XRPD in the 2 theta range 13° – 22°, by using Cu Kα radiation (λ = 1.54060 Å), is actually a phase transition as revealed by the pattern acquired over a wider angular range.

Figures 10S-a and b show the transformation of microcrystalline **CUT-1** into a different unknown phase monitored by time-resolved powder X-ray diffraction experiments at GILDA-BM08 at ESRF (Grenoble) using a fixed wavelength of 0.687797 Å.

The sample was dried under vacuum conditions at 50°C and packed into a 0.8 mm diameter glass capillary. The dehydrated powder was then maintained exposed to the vapour of nitromethane by placing carefully a drop of solvent just above the sample and sealing the capillary with wax.

Powder diffraction patterns were recorded on a 2 mm slit-delimited portion of a translating flat image plate IP detector for four hours at a constant translation speed and a time resolution of 100 seconds.[9,10] The obtained 2-D images were processed by integrating the vertical stripes using FIT2D software[11] to produce 1D diffraction patterns.

1 Bruker, *SAINT+*, 2007, Bruker AXS Inc., Madison, Wisconsin, USA.
2 Bruker, *APEX II*, 2009, Bruker AXS Inc., Madison, Wisconsin, USA.
3 M. C. Burla, R. Caliandro, M. Camalli, B. Carrozzini, G. L. Cascarano, L. De Caro, C. Giacovazzo, G. Polidori and R. Spagna, *J. Appl. Crystallogr.*, 2005, **38**, 381–388.
4 G. M. Sheldrick, *Acta Crystallogr. Sect. C Struct. Chem.*, 2015, **71**, 3–8.
5 L. J. Farrugia, *J. Appl. Crystallogr.*, 2012, **45**, 849–854.
6 A. L. Spek, *Acta Crystallogr. Sect. C Struct. Chem.*, 2015, **71**, 9–18.
7 R. G. Xiong, C. M. Liu, J. L. Zuo and X. Z. You, *Inorg. Chem. Commun.*, 1999, **2**, 292–297.
8 L. Carlucci, N. Cozzi, G. Ciani, M. Moret, D. M. Proserpio and S. Rizzato, *Chem. Commun. (Cambridge, United Kingdom)*, 2002, 1354–1355.
9 P. Norby, *J. Appl. Crystallogr.*, 1997, **30**, 21–30.
10 C. Meneghini, G. Artioli, A. Balerna, A. F. Gualtieri, P. Norby and S. Mobilio, *J. Synchrotron Radiat.*, 2001, **8**, 1162–1166.
11 A. P. Hammersley, S. O. Svensson, M. Hanfland, A. N. Fitch and D. Hausermann, *High Press. Res.*, 1996, **14**, 235–248.